Appendix

Linear Interference Suppression Detection to the FHSS and DSSS Coexistent Environment in the Same Frequency Band

Cha'o-Ming Chang and Kwang-Cheng Chen

Abstract

In this paper, a multiuser detection scheme considering the presence of direct sequence spread spectrum (DSSS) interferences and frequency hopping spread spectrum (FHSS) interferences is proposed whose complexity grows linearly to the number of interference sources. Such an approach extends the ability of conventional linear multiuser detection to demodulate non-linear modulated signal (e.g GFSK). In addition, it can be used on both the 802.11b and Bluetooth devices to enhance their coexistence ability.

1 Introduction

Driven by the great amount of interests in developing the wireless personal area network (WPAN), the IEEE 802.15 working group was formed working on the standard that provides low-cost, low-power consumption and short-distance (around 10 meters) transmission. To ease the development, the IEEE 802.15 working group accepted the suggestion of Bluetooth Special Interest Group to incorporate Bluetooth technology into the 802.15 standard, known as IEEE 802.15.1. However, the usage of Bluetooth technology on the unlicensed 2.4 GHz band which is also the transmission band for many communications systems (e.g. IEEE WLAN 802.11b, and HomeRF) suggests the problem of mutual interference from these incompatible protocols.

To seek a solution, the IEEE 802.15.2 task group was formed to work on the coexistence issue between these protocols. Especially, the coexistence between IEEE WLAN 802.11b and Bluetooth is of primary importance. As the 802.11b employed the direct sequence spread spectrum (DSSS) transmission technology while the Bluetooth employed frequency hopping

1

spread spectrum (FHSS) technology, we are dealing the problem of detecting a DSSS or FHSS signal interfered by multiple DSSS and FHSS interference.

A great amount of work was done on the the interference suppression for the DSSS signal by its inherited ability to suppress interference [1, 2, 3]. On the other hand, the FHSS signal mitigates the interference by employing proper adaptive frequency hopping mechanisms [4]. Both categories of these known interference suppression techniques utilize the interference suppression nature of spread spectrum communications by ignoring the possible information from interference.

Since 1986 [5], a new series of designs known as multiuser detectors were proposed to mitigate the multiple access interference (MAI) derived from the simultaneously received DSSS signals in the same frequency band. Among these known multiuser detectors, the linear-complexity multiuser detectors [6, 7, 8] designed according to different design criteria do effectively mitigate the interference. However, these designs were designed to suppress the DSSS interference only.

In the detection of a direct sequence spread spectrum (DSSS) or frequency hopping spread spectrum (FHSS) signal interfered by other DSSS and FHSS signals, the optimal detection based on the *maximum a posteriori* probability (MAP) criterion could be derived similarly as in multiuser detection [5]. Despite the optimal performance such an interference suppression detector stands, its dramatically increased complexity to the number of interference sources suggests the need of a linear-complexity interference suppression detector which effectively suppresses the interference. Previous development on linear multiuser detection is subjected to the linearly modulated signals, such as the M-ary phase shift keying (MPSK) modulation. In the sequel, we shall extend the development to non-linear modulated signals. In particular, to meet the specifications in IEEE 802.11b and Bluetooth, we develop the linear-complexity interference suppression detectors considering both the presence of DSSS signals modulated by BPSK (or QPSK) and the FHSS signals modulated by Gaussian frequency shift keying (GFSK).

2

The rest of the paper is organized as: In Section 2, the assumptions and signal model used are defined. In Section 3, the general design of linear-complexity interference suppression detection for the DSSS signal is proposed considering the presence of other DSSS and FHSS signals. Section 4 elaborates the design of linear-complexity interference suppression detection for the FHSS signal interfered by other FHSS and/or DSSS signals in a general way. Section 5 presents the applications of previous sections in the Bluetooth and IEEE 802.11b coexistent environment and we make the conclusions in Section 6.

2 Signal Model and Assumptions

To ease the development, we assume that the number of interfered DSSS and FHSS signals, their used signature waveforms, and carrier frequencies are known to the receiver. In addition, the received timings, carrier phases, and amplitudes of all the received signals are also available. We also consider the additive white Gaussian noise (AWGN) channel, although the more practical scenarios such as the multi-path fading channels could be easily extended with our development. Let $s_k(t)$ denote the signature waveform of the kth DSSS signal.

$$s_k(t) = \sum_{n=1}^{N_c-1} p_k(n)u(t-nT_c), \tag{1}$$

where N_c is the number of chips; $p_k(n)$ for $n = 0, 1, \cdots, N_c - 1$ represents the signature sequence of user k; $u(t)$ is the pulse shape function with support $[0, T_c)$; and T_c is the chip time. The received signal containing K DSSS signals and L FHSS signals is therefore

$$r(t) = \sum_{m=0}^{M-1} \sum_{k=1}^{K} b_k^{(DS)}(m)s_k(t-\tau_k^{(DS)}-mT)\rho_k^{(DS)}cos(\omega_0 t + \phi_k^{(DS)})$$

$$+ \sum_{l=1}^{L} \rho_l^{(FH)}(t-\tau_l^{(FH)})cos(\omega_l t + 2\pi h \sum_{n=0}^{N-1} b_l^{(FH)}(n)q(t-\tau_l^{(FH)}-nT) + \phi_l^{(FH)}) + z(t),$$

$$\tag{2}$$

where M and N denote the length of DSSS signals and FHSS signals respectively; $b_k^{(DS)}(m)$[1] for $m = 0, 1, \cdots, M - 1$ and $b_l^{(FH)}(n)$ for $n = 0, 1, \cdots, N - 1$ are the information sequences of the kth DSSS signal and the lth FHSS signal respectively; $\rho_k^{(DS)}$ and ω_0 represent the received amplitude and carrier frequency of the kth DSSS signal; $\phi_k^{(DS)}$ and $\phi_l^{(FB)}$ stand for the received carrier phase of the kth DSSS signal and the received initial phase of the ith FHSS signal; ω_l denotes the lth and carrier frequency of the FHSS signal; T is the symbol duration; $z(t)$ is the additive white Gaussian noise;

$$\rho_l^{(FB)}(t) = \begin{cases} \rho_l^{(FH)} & \text{for } t >= 0 \\ 0 & \text{otherwise} \end{cases}$$

denotes the lth received amplitude of FHSS signal; h and $q(t)$ stand for the modulation index and the Gaussian filtered pulse shape function of the GFSK signal; and $\tau_k^{(DS)}$ and $\tau_l^{(FH)}$ are the received timings of the kth DSSS signal and the lth FHSS signal respectively.

3 Linear Interference Suppression Detection for DSSS signals

Assume the desired information is carried by the first signature waveform $s_1(t)$ among the DSSS signals, and its received timing is 0. (i.e. $\tau_1^{(DS)} = 0$.)

3.1 Synchronous Interference Suppression: A special case

To ease the illustrations, we temporarily start our development from the synchronous case. That is, we assume $\tau_k^{(DS)} = \tau_l^{(FH)} = 0$ for all k and l. With this assumption, one-shot interference suppression detection is easier to be implemented.

Because GFSK is a non-linearly modulated approach, its signal when transmitting a "1" is not a scalar multiplication of the signal when transmitting a "0". However, by approxi-

---

[1] $b_k^{(DS)}(m)$ may but not limit to $\{-1, 1\}$ considering other linear modulating approaches. e.g. M-ary PSK and QAM modulations. However, to ease the interpretation and without loss of generality, we consider the BPSK modulation in the sequel.

mating[2] $q(t)$ as

$$q(t) = \begin{cases} 0 & \text{for } t \leq 0 \\ 1/2 & \text{for } t \geq T \end{cases} ,$$

we can interpret the received lowpass equivalent signal as

$$r_{LP}(t) = \sum_{m=0}^{M-1} \sum_{k=1}^{K} b_k^{(DS)}(m) \rho_k^{(DS)} e^{j\phi_k^{(DS)}} s_k(t - mT)$$

$$+ \sum_{n=0}^{N-1} \sum_{l=1}^{L} [\rho_{2l-1}^{(FH)}(n) s_{K+2l-1}(t - nT) + \rho_{2l}^{(FH)}(n) s_{K+2l}(t - nT)] + z_{LP}(t), \tag{3}$$

where

$$s_{K+2l-1}(t) = \begin{cases} e^{j[(\omega_l - \omega_0)t + 2\pi h q(t)]} & \text{for } t \in [0, T) \\ 0 & \text{otherwise} \end{cases} ; \tag{4}$$

$$s_{K+2l}(t) = \begin{cases} e^{j[(\omega_l - \omega_0)t - 2\pi h q(t)]} & \text{for } t \in [0, T) \\ 0 & \text{otherwise} \end{cases} ; \tag{5}$$

$$\rho_{2l-1}^{(FH)}(n) = \begin{cases} \rho_l^{(FH)} e^{j[\phi_l^{(FH)} + \pi h \sum_{a=0}^{n-1} b_l^{(FH)}(a)]} & \text{if } b_l^{(FH)}(n) = 1 \\ 0 & \text{otherwise} \end{cases} ; \tag{6}$$

$$\rho_{2l}^{(FH)}(n) = \begin{cases} \rho_l^{(FH)} e^{j[\phi_l^{(FH)} + \pi h \sum_{a=0}^{n-1} b_l^{(FH)}(a)]} & \text{if } b_l^{(FH)}(n) = -1 \\ 0 & \text{otherwise} \end{cases} ; \tag{7}$$

$b_l^{(FH)}(n) = 0$ for $n < 0$; $j \equiv \sqrt{-1}$; and $z_{LP}(t)$ is the lowpass equivalent waveform of $z(t)$. Such an interpretation can be considered as a linearization approach which transforms a system of L non-linearly modulated signals into a system of $2L$ linearly modulated signals.

The sufficient statistics to detect the mth bits of the desired DSSS signal are therefore

$$\underline{r}(m) \equiv \begin{bmatrix} \int_{mT}^{(m+1)T} r_{LP}(t) s_1(t - mT) dt \\ \int_{mT}^{(m+1)T} r_{LP}(t) s_2(t - mT) dt \\ \vdots \\ \int_{mT}^{(m+1)T} r_{LP}(t) s_K(t - mT) dt \\ \int_{mT}^{(m+1)T} r_{LP}(t) s_{K+1}(t - mT) dt \\ \int_{mT}^{(m+1)T} r_{LP}(t) s_{K+2}(t - mT) dt \\ \vdots \\ \int_{mT}^{(m+1)T} r_{LP}(t) s_{K+2L}(t - mT) dt \end{bmatrix} , \tag{8}$$

---

[2]A more accurate approximation could be obtained by

$$q(t) = \begin{cases} 0 & \text{for } t \leq -\epsilon T \\ 1/2 & \text{for } t \geq (\epsilon + 1)T \end{cases} ,$$

for some non-negative integer ϵ. And a corresponding equalizer to mitigate the introduced inter-symbol interference (ISI) would be desired.

for $m = 0, 1, \cdots, M - 1$. And

$$
\underline{r}(m) = \mathbf{R}
\begin{bmatrix}
b_1^{(DS)}(m)\rho_1^{(DS)}e^{j\phi_1^{(DS)}} \\
b_2^{(DS)}(m)\rho_2^{(DS)}e^{j\phi_2^{(DS)}} \\
\vdots \\
b_K^{(DS)}(m)\rho_K^{(DS)}e^{j\phi_K^{(DS)}} \\
\rho_1^{(FH)}(m) \\
\rho_2^{(FH)}(m) \\
\vdots \\
\rho_L^{(FH)}(m)
\end{bmatrix}
+
\begin{bmatrix}
\int_{mT}^{(m+1)T} z(t)s_1(t - mT)dt \\
\int_{mT}^{(m+1)T} z(t)s_2(t - mT)dt \\
\vdots \\
\int_{mT}^{(m+1)T} z(t)s_K(t - mT)dt \\
\int_{mT}^{(m+1)T} z(t)s_{K+1}(t - mT)dt \\
\int_{mT}^{(m+1)T} z(t)s_{K+2}(t - mT)dt \\
\vdots \\
\int_{mT}^{(m+1)T} z(t)s_{K+2L}(t - mT)dt
\end{bmatrix},
\qquad (9)
$$

where $\mathbf{R}$ is the $(K + 2L) \times (K + 2L)$ matrix whose entry in kth row and lth column is $\int_0^T s_l(t)s_k^*(t)dt$ and the superscript $*$ denotes the complex conjugate operation.

$\mathbf{R}$ is nonsingular if the $K + 2L$ functionals $\{s_k(t)|k = 1, 2, \cdots, K + 2L\}$ are linearly independent. Such an independence assumption always sustains unless the employed signature waveforms are constant functions, which does not happen in the practical applications. Therefore, the linear-complexity interference suppression detector to retrieve the desired DSSS information bits is (see Figure 1)

$$
\hat{b}_1^{(DS)}(m) = sgn\{e^{-j\phi_1^{(DS)}}\underline{A}_1^t\underline{r}(m)\}; \text{ for } m = 0, 1, \cdots, M - 1, \qquad (10)
$$

where the superscript t denotes the transpose operation; $\underline{A}_k^t$ represents the kth row vector of the $(K + 2L) \times (K + 2L)$ matrix $\mathbf{A}$; and $\mathbf{A}$ is obtained by either

1. De-correlating type:

    $\mathbf{A} = \mathbf{R}^{-1}$ or

2. Linear minimum mean square error (LMMSE) type:

    $\underline{A}_1^t = arg \ \min_{\underline{d}^t} |\underline{d}^t\underline{r}(m) - b_1^{(DS)}(m)\rho_1^{(DS)}e^{j\phi_1^{(DS)}}|$

Remark: $\underline{A}_1^t$ could be calculated beforehand in the de-correlating type case to simplify the implementation.
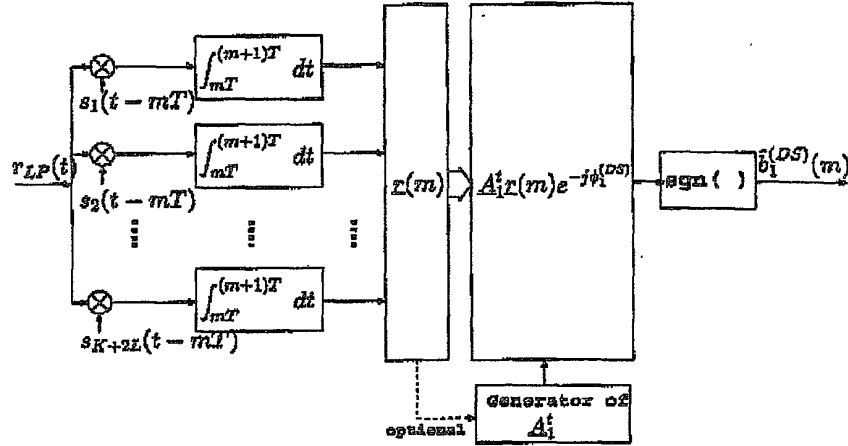
Figure 1: Block diagram of interference suppression detectors for the DSSS signal: synchronous case.

3.2 Asynchronous Interference Suppression

It is known in the multiuser detection that an asynchronous system with K users transmitting M information bits could be considered as a synchronous system with MK users [6]. However, we shall development a further simplified scheme.

To give a clearer illustration, without loss of generality, we assume that the DSSS signals are synchronous, while the FHSS signals are asynchronous. Our rationale to implement the one-shot detection in the asynchronous channel could be explained by Figure 2 to split an asynchronous waveform into two synchronous waveforms [9]. For example, $s_{K+2l-1}(t-\tau_l^{(FH)})$ is split into a linear combination of $s_{K+2l-1}^{(0)}(t)$ and $s_{K+2l-1}^{(1)}(t)$, where

$$s_{K+2l-1}^{(0)}(t) = \begin{cases} s_{K+2l-1}(t+T-\tau_l^{(FH)}) & \text{for } t \in [0, \tau_l^{(FH)}) \\ 0 & \text{otherwise} \end{cases} \text{, and} \tag{11}$$

$$s_{K+2l-1}^{(1)}(t) = \begin{cases} s_{K+2l-1}(t-\tau_l^{(FH)}) & \text{for } t \in [\tau_l^{(FH)}, T) \\ 0 & \text{otherwise} \end{cases} \text{.} \tag{12}$$
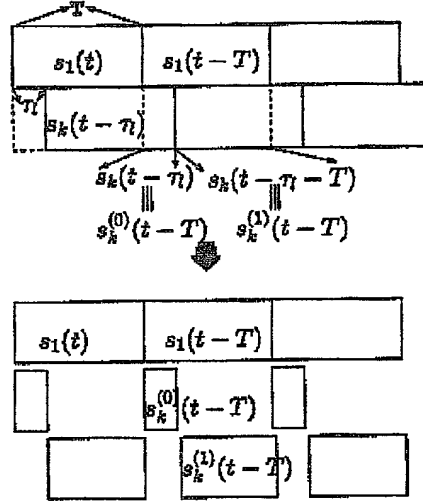
7

Figure 2: The procedure to split a waveform $s_k(t-\tau_l)$ to two waveforms to realize synchronous links.

Similarly, $s_{K+2l}(t-\tau_l^{(FH)})$ is considered as a linear combination of $s_{K+2l}^{(0)}(t)$ and $s_{K+2l}^{(1)}(t)$ with

$$s_{K+2l}^{(0)}(t) = \begin{cases} s_{K+2l}(t+T-\tau_l^{(FH)}) & \text{for } t \in [0, \tau_l^{(FH)}) \\ 0 & \text{otherwise} \end{cases} \quad, \text{ and} \qquad (13)$$

$$s_{K+2l}^{(1)}(t) = \begin{cases} s_{K+2l}(t-\tau_l^{(FH)}) & \text{for } t \in [\tau_l^{(FH)}, T) \\ 0 & \text{otherwise} \end{cases} \quad, \qquad (14)$$

for $l = 1, 2, \cdots, L$.

Thus the corresponding linear interference suppression detection is

$$\hat{b}_1^{(DS)}(m) = sgn\{e^{-j\phi_1^{(DS)}} \underline{A}_1^t \underline{r}(m)\}; \text{ for } m = 0, 1, \cdots, M-1, \qquad (15)$$

8

where

$$
\underline{r}(m) \equiv \begin{bmatrix}
\int_{mT}^{(m+1)T} r_{LP}(t)s_1(t-mT)dt \\
\int_{mT}^{(m+1)T} r_{LP}(t)s_2(t-mT)dt \\
\vdots \\
\int_{mT}^{(m+1)T} r_{LP}(t)s_K(t-mT)dt \\
\int_{mT}^{(m+1)T} r_{LP}(t)s_{K+1}^{(0)}(t-mT)dt \\
\int_{mT}^{(m+1)T} r_{LP}(t)s_{K+1}^{(1)}(t-mT)dt \\
\int_{mT}^{(m+1)T} r_{LP}(t)s_{K+2}^{(0)}(t-mT)dt \\
\int_{mT}^{(m+1)T} r_{LP}(t)s_{K+2}^{(1)}(t-mT)dt \\
\vdots \\
\int_{mT}^{(m+1)T} r_{LP}(t)s_{K+2L}^{(0)}(t-mT)dt \\
\int_{mT}^{(m+1)T} r_{LP}(t)s_{K+2L}^{(1)}(t-mT)dt
\end{bmatrix}
\tag{16}
$$

is a $(K+4L) \times 1$ column vector and $\underline{A}_1^t$ is the first row vector of the $(K+4L) \times (K+4L)$ matrix A which is designed similarly as in the synchronous case.

Remark: Although we linearly combine the $K+4L$ sufficient statistics in the asynchronous environment, the number of needed match filters could be reduced to $K+2L$ as in the synchronous case. This is mainly because that $s_{K+l}^{(0)}(t)$ and $s_{K+l}^{(1)}(t)$ are non-overlapped functionals, which will be elaborated in Section 5.

4 Linear Interference Suppression Detection on FHSS Signals

4.1 FHSS Signals Do Not Collide

To ease the development, we temporarily assume that the FHSS signals do not collide in the same frequency band. Such an assumption is reasonable for only a moderate number of FHSS signals concurrently transmitted.

On the detection of the FHSS signal, a narrow-band passband filter to retrieve the desired FHSS signal is used as in Figure 3, and therefore the received lowpass equivalent signal can
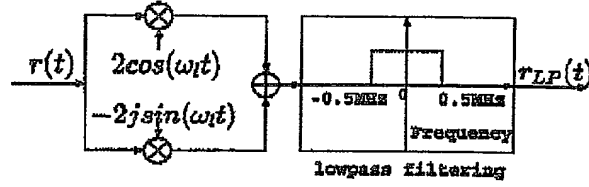
Figure 3: Block diagram to obtain received lowpass equivalent signal $r_{LP}(t)$ considering the FHSS signal with bandwidth 1 MHz.

be written as

$$
\begin{aligned}
r_{LP}(t) &= \sum_{m=0}^{M-1} \sum_{k=1}^{K} b_k^{(DS)}(m) \tilde{s}_k(t - \tau_k^{(DS)} - mT) \rho_k^{(DS)} e^{j\phi_k^{(DS)}} \\
&\quad + \sum_{n=0}^{N-1} [\rho_1^{(FH)}(n)\tilde{s}_{K+1}(t - nT) + \rho_2^{(FH)}(n)\tilde{s}_{K+2}(t - nT)] + z_{LP}(t),
\end{aligned}
\tag{17}
$$

where $\tilde{s}_k(t)$ for $k = 1, 2, \cdots, K$ are the filtered signal of the signature waveforms $s_k(t)$;

$$
\tilde{s}_{K+1}(t) = \begin{cases} e^{j2\pi h q(t)} & \text{for } t \in [0, T) \\ 0 & \text{otherwise} \end{cases} ;
\tag{18}
$$

$$
\tilde{s}_{K+2}(t) = \begin{cases} e^{-j2\pi h q(t)} & \text{for } t \in [0, T) \\ 0 & \text{otherwise} \end{cases} ;
\tag{19}
$$

and the other parameters were defined previously. Similarly, by defining

$$
\tilde{s}_k^{(0)}(t) = \begin{cases} \tilde{s}_k(t + T - \tau_k^{(DS)}) & \text{for } t \in [0, \tau_k^{(DS)}) \\ 0 & \text{otherwise} \end{cases} \quad \text{and}
\tag{20}
$$

$$
\tilde{s}_k^{(1)}(t) = \begin{cases} \tilde{s}_k(t - \tau_k^{(DS)}) & \text{for } t \in [\tau_k^{(DS)}, T) \\ 0 & \text{otherwise} \end{cases} ,
\tag{21}
$$

$$
\tag{22}
$$

for $k = 1, 2, \cdots, K$, $\tilde{s}_k(t - \tau_k^{(DS)})$ could be considered as a linear combination of $\tilde{s}_k^{(0)}(t)$ and $\tilde{s}_k^{(1)}(t)$. The communications system with K asynchronous DSSS signals and 1 FHSS signal is equivalent to a communications system with $2K$ DSSS signals and 2 FHSS signals.

Therefore, by forming the sufficient statistics

$$
\underline{r}(n) = \begin{bmatrix}
\int_{nT}^{(n+1)T} r_{LP}(t)\tilde{s}_1^{(0)}(t-nT)dt \\
\int_{nT}^{(n+1)T} r_{LP}(t)\tilde{s}_1^{(1)}(t-nT)dt \\
\int_{nT}^{(n+1)T} r_{LP}(t)\tilde{s}_2^{(0)}(t-nT)dt \\
\int_{nT}^{(n+1)T} r_{LP}(t)\tilde{s}_2^{(1)}(t-nT)dt \\
\vdots \\
\int_{nT}^{(n+1)T} r_{LP}(t)\tilde{s}_K^{(0)}(t-nT)dt \\
\int_{nT}^{(n+1)T} r_{LP}(t)\tilde{s}_K^{(1)}(t-nT)dt \\
\int_{nT}^{(n+1)T} r_{LP}(t)\tilde{s}_{K+1}(t-nT)dt \\
\int_{nT}^{(n+1)T} r_{LP}(t)\tilde{s}_{K+2}(t-nT)dt
\end{bmatrix}
\tag{23}
$$

The one-shot linear interference suppression detection is

$$
\hat{b}_1^{(FH)}(n) = sng\{|\underline{A}_{2K+1}^t \underline{r}(n)| - |\underline{A}_{2K+2}^t \underline{r}(n)|\}; \text{ for } n = 0, 1, \cdots, N-1,
\tag{24}
$$

where $\underline{A}_k^t$ denotes the kth row vector of the $(2K+2) \times (2K+2)$ matrix A which is designed according to the similar criteria in the previous section.

Please note that $\underline{A}_{2K+1}^t \underline{r}(n)$ and $\underline{A}_{2K+2}^t \underline{r}(n)$ are the estimates of $\rho_1^{(FH)}(n)$ and $\rho_2^{(FH)}(n)$ respectively, which contain the summation of previously transmitted information bits. This side information shall suggest better detection designs (by constructing the trellis diagram to utilize the characteristics of GFSK modulation with memory) at the cost of increased complexity.

4.2   General Case that FHSS Signals Collide

When the number of devices employing FHSS transmission increases, the transmitted FHSS signals from different devices might hop on the same frequency band and cause severe interference, especially when the devices are synchronized.

In this subsection, we extend the ability of our proposed linear interference suppression detection for FHSS signals to the scenario that more than one FHSS signal hop onto the same frequency band. The filtered received lowpass equivalent signal with K DSSS interference

signals and L FHSS signals in the same frequency band is thus

$$
\begin{aligned}
r_{LP}(t) = & \sum_{m=0}^{M-1} \sum_{k=1}^{K} b_k^{(DS)}(m) \tilde{s}_k(t - \tau_k^{(DS)} - mT) \rho_k^{(DS)} e^{j\phi_k^{(DS)}} + z_{LP}(t) \\
& + \sum_{n=0}^{N-1} \sum_{l=1}^{L} [\rho_{2l-1}^{(FH)}(n) \tilde{s}_{K+1}(t - \tau_l^{(FH)} - nT) + \rho_{2l}^{(FH)}(n) \tilde{s}_{K+2}(t - \tau_l^{(FH)} - nT)]
\end{aligned}
\tag{25}
$$

where all the variables were defined previously. Without loss of generality, suppose that the desired FHSS signal is the first one and its received timing is 0. That is, $\tau_1^{(FH)} = 0$. To implement one-shot detection with lower complexity, we consider $\tilde{s}_{K+1}(t - \tau_l^{(FH)})$ and $\tilde{s}_{K+2}(t - \tau_l^{(FH)})$ as the linear combination of $\{\tilde{s}_{K+2l-1}^{(i)}(t) | \; i = 0, 1\}$ and $\{\tilde{s}_{K+2l}^{(i)}(t) | \; i = 0, 1\}$ respectively, for $l = 2, \cdots, L$. And thus the sufficient statistics are the entries of

$$
\underline{r}(n) = \begin{bmatrix}
\int_{nT}^{(n+1)T} r_{LP}(t) \tilde{s}_1^{(0)}(t - nT) dt \\
\int_{nT}^{(n+1)T} r_{LP}(t) \tilde{s}_1^{(1)}(t - nT) dt \\
\int_{nT}^{(n+1)T} r_{LP}(t) \tilde{s}_2^{(0)}(t - nT) dt \\
\int_{nT}^{(n+1)T} r_{LP}(t) \tilde{s}_2^{(1)}(t - nT) dt \\
\vdots \\
\int_{nT}^{(n+1)T} r_{LP}(t) \tilde{s}_K^{(0)}(t - nT) dt \\
\int_{nT}^{(n+1)T} r_{LP}(t) \tilde{s}_K^{(1)}(t - nT) dt \\
\int_{nT}^{(n+1)T} r_{LP}(t) \tilde{s}_{K+1}(t - nT) dt \\
\int_{nT}^{(n+1)T} r_{LP}(t) \tilde{s}_{K+2}(t - nT) dt \\
\int_{nT}^{(n+1)T} r_{LP}(t) \tilde{s}_{K+3}^{(0)}(t - nT) dt \\
\int_{nT}^{(n+1)T} r_{LP}(t) \tilde{s}_{K+3}^{(1)}(t - nT) dt \\
\vdots \\
\int_{nT}^{(n+1)T} r_{LP}(t) \tilde{s}_{K+2L-1}^{(0)}(t - nT) dt \\
\int_{nT}^{(n+1)T} r_{LP}(t) \tilde{s}_{K+2L}^{(1)}(t - nT) dt
\end{bmatrix}
\tag{26}
$$

which is an complex-valued $(2K + 4L - 2) \times 1$ column vector. And the one-shot linear interference suppression detection is

$$
\hat{b}_1^{(FH)}(n) = sng\{|\underline{A}_{2K+1}^t \underline{r}(n)| - |\underline{A}_{2K+2}^t \underline{r}(n)|\}; \quad \text{for } n = 0, 1, \cdots, N-1,
\tag{27}
$$

where $\underline{A}_k^t$ denotes the kth row vector of the $(2K + 4L - 2) \times (2K + 4L - 2)$ matrix A which is designed according to the similar criteria in previous section.

Remarks:

12

IPC Confidential

1. The effectiveness of the proposed linear interference suppression detection is ensured by the linear independence of the used DSSS and FHSS signals.

2. Both the de-correlating and minimum mean square criteria suggest effective linear combinations on the sufficient statistics to successfully suppress the interference.

3. As mentioned in previous section, the number of match filters to implement the linear interference suppression detection with K DSSS signals and L FHSS signals is $K+2L$.

5 IEEE 802.11b and Bluetooth Coexistent Environment: An example

Previous section elaborated the linear-complexity interference suppression detection considering the interference from a couple of DSSS and/or FHSS signals in a generalized way. In the sequel, we shall demonstrate its applications with practical considerations.

5.1 Linear Interference Suppression Detection on Bluetooth Devices

Because of the carrier sensing mechanism implemented on the IEEE 802.11b devices, we could ignore the occasions that multiple DSSS signals transmitted in the same frequency band. That is, we only consider $K=1$ as in previous development. In addition, since the FHSS signals hop over a wide range of frequency bands (79 bands), the probability that more than one FHSS signal hop in the same frequency band is small, for a moderate number of Bluetooth piconets. And therefore, $L=1$.

We further consider the DSP-based (digital signal processor) implementation. With these practical considerations, the received lowpass equivalent signal $r_{LP}(t)$ is

$$
\begin{aligned}
r_{LP}(t) = &\sum_{m=0}^{M-1} b^{(DS)} \tilde{s}_1(t - \tau^{(DS)} - mT) \rho^{(DS)} e^{j\phi^{(DS)}} + z_{LP}(t) \\
&+ \sum_{n=0}^{N-1} [\rho_1^{(FH)}(n) \tilde{s}_2(t-nT) + \rho_2^{(FH)}(n) \tilde{s}_3(t-nT)],
\end{aligned}
\tag{28}
$$

13

where we drop the subscript $_1$ regarding the DSSS signal to make the presentation clearer.

According to the sampling theorem, we sample $r_{LP}(t)$ at the rate $1/T_s \equiv 2/T$ and obtain the sequence

$$
\begin{aligned}
r(n,i) &\equiv r_{LP}(nT + iT_s + \tau) \\
&= \rho^{(DS)}e^{j\phi^{(DS)}}b^{(DS)}(n - d_{1,i})\tilde{s}_1((iT_s + \tau - \tau^{(DS)})_T) \\
&\quad + \rho_1^{(FH)}(n)\tilde{s}_2((iT_s + \tau)_T) + \rho_2^{(FH)}(n)\tilde{s}_3((iT_s + \tau)_T) \\
&\quad + z(n,i),
\end{aligned}
\tag{29}
$$

where $z(n,i) \equiv z_{LP}(nT+iT_s+\tau)$; τ is the known misalignment ($\tau \in [0, T_s)$); $(\cdot)_T \equiv (\cdot) \bmod T$; and $d_{1,i} = \beta$ provided $-\beta T \leq iT_s + \tau - \tau^{(DS)} < (1-\beta)T$.

The corresponding block diagram applying our previously proposed linear interference suppression detection is
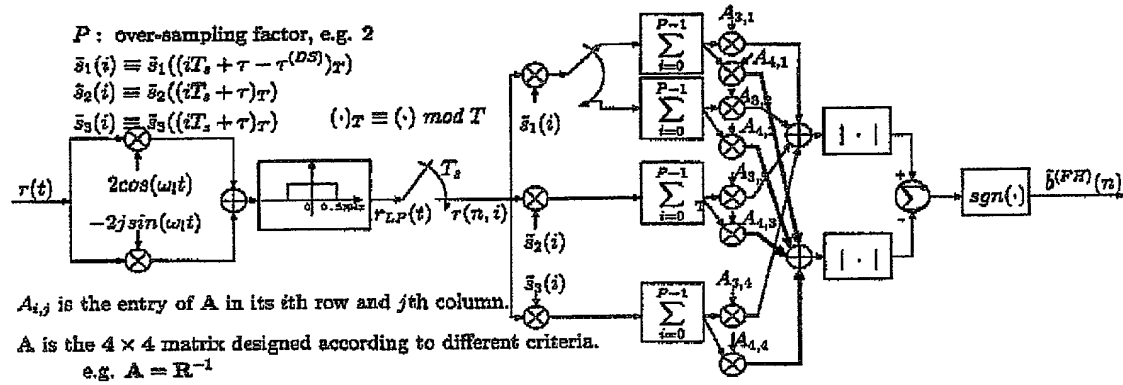

Figure 4: Block diagram of linear interference suppression detection on Bluetooth devices.

As in Figure 4, the number of correlators required on the Bluetooth devices is 3, and the combination coefficients $\{A_{3,l}, A_{4,l} | $ for $ l = 1, 2, 3, 4.\}$ could be pre-determined if applying the decorrelating-type design criterion, which suggests an effective but simple design.

In fact, a complete receiver design in the IEEE 802.11b and Bluetooth coexistent environment includes not only the interference suppression detection, but also an identification
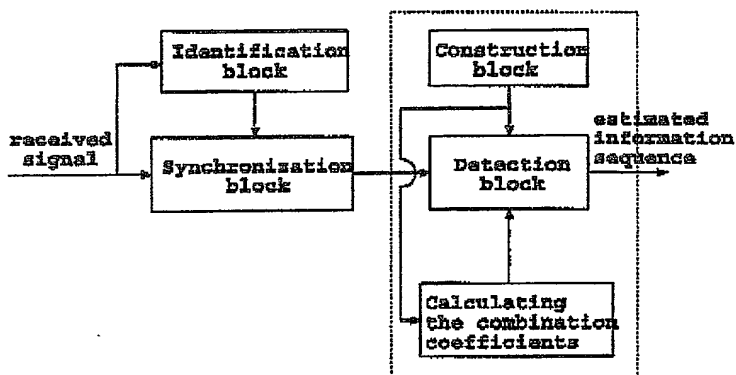
14

Figure 5: Block diagram of the receiver in the IEEE 802.11b and Bluetooth coexistent environment.

block and a synchronization block to identify the number of DSSS and FHSS interferences, to identify the employed signature sequences of the DSSS signals, and to estimate the received timings, phases, and amplitudes of all the received DSSS and FHSS signals respectively. In Figure 5, the *Construction block* is used to construct extra signals (as the signals in (4) and (5)) such that an employed non-linearly modulated signal is the linear combination of some linearly modulated signals as in the brackets of (3). The *Detection block* correlates the received signal to form the sufficient statistics and further linearly combine these sufficient statistics according to the design criterion. That is, Figure 4 represents the dashed box in Figure 5 for Bluetooth devices. And it remains to design the *Identification block* and the *Synchronization block*.

In [10], a series of synchronizers to estimate the received timings, phases, and amplitudes of simultaneously transmitted DSSS signals was proposed with feasible complexity. However, considering the practical Bluetooth and IEEE 802.11b coexistent environment, some simpler designs are possible.

Our first design utilizing the asynchronous nature between the 802.11b and Bluetooth devices is illustrated by Figure 6 to possibly estimate the received timing, phase and amplitude of DSSS interference before the reception of the desired FHSS signal. With the knowledge
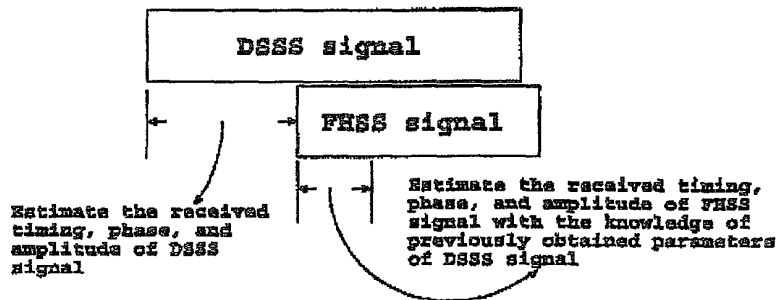
15

Figure 6: Diagram demonstrating the rationale behind our proposed synchronization mechanism.

of the previously estimated synchronization parameters of the DSSS signal, it is easier to retrieve the received timing, phase, and amplitude of the FHSS signal interfered by the DSSS signal.
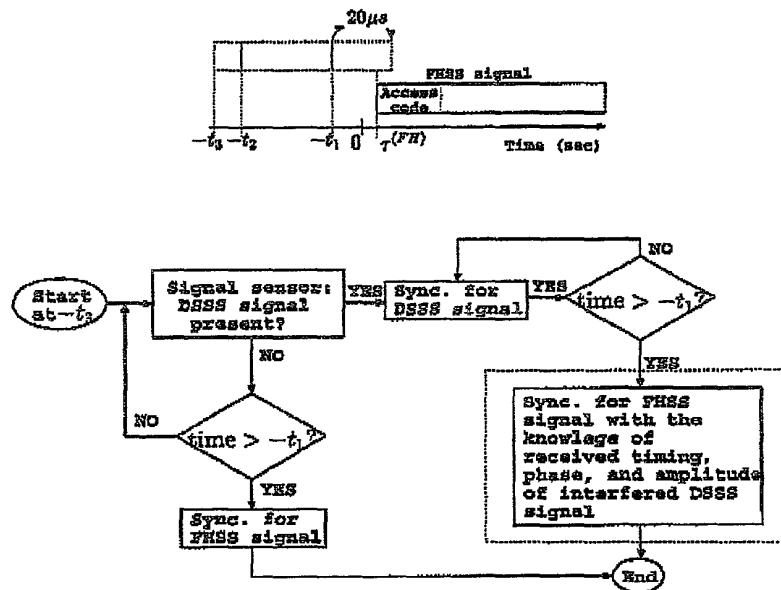

Figure 7: Flow diagram of the Bluetooth synchronization block.

16

The flow diagram is shown in Figure 7, where $t_2 - t_1$ is the time required to estimate the received timing, phase, and amplitude of the DSSS signal; and the time period $[-10\mu \sec, 10\mu \sec]$ as specified in [11] is the period of uncertainty that the Bluetooth packet is received. The synchronization mechanism operates as below:

Step 1: The receiver of Bluetooth device starts to detect the presence of the DSSS signal by the *Signal sensor* at time $-t_3$.

Step 2: If the *Signal sensor* detects the presence of the DSSS signal, the synchronizer as in point-to-point DSSS communications systems is performed to estimate the received timing, phase, and amplitude of the DSSS signal. These estimated information is then utilized to retrieve the received timing, phase, and amplitude of the desired FHSS signal as shown in the dashed box of Figure 7.

Step 3: If the *Signal sensor* does not sense the DSSS signal after time $-t_1$, the synchronizer as in point-to-point FHSS communications systems is employed to estimate the received timing, phase, and amplitude of the FHSS signal.

Remarks:

- If the *Signal sensor* detects the presence of the DSSS signal after time $-t_2$, the performance of the proposed synchronization mechanism will be degraded.

- Such a synchronization mechanism ignores the possibility that the DSSS signal is received after time $-t_1$, and thus might also degrades its performance.

- However, if the implemented carrier sensing mechanism in IEEE 802.11b can sense the presence of the FHSS signal transmitted by the Bluetooth devices, the previously described performance degradation could be alleviated.

- Such a synchronization mechanism can be easily implemented on the current Bluetooth specifications [11] without any modifications and could be considered as the ready design.

As mentioned in Step 2, we need to design the synchronization scheme for the FHSS signal in the presence of the DSSS signal with the knowledge of the received timing, phase, and amplitude of the DSSS signal and the information bits of the FHSS signal by the access code of the Bluetooth packet (the dashed box in Figure 7).

Assume a coarse timing estimation is available such that the received timing of the FHSS signal is within an uncertainty of $T_s (\equiv T/2)$. Without loss of generality, we assume that the unknown received timing $\tilde{\tau}^{(FH)} \in (-T_s, 0]$. The received lowpass equivalent signal $r_{LP}(t)$ sampled at rate $1/T_s$ could be written as

$$
\begin{aligned}
r(n,i) &\equiv r_{LP}(nT + iT_s) \\
&= \rho^{(DS)} e^{j\phi^{(DS)}} \tilde{b}^{(DS)}(n - d_{1,i}) \tilde{s}_1((iT_s - \tau^{(DS)})_T) + z(n,i) \\
&\quad + \tilde{\rho}^{(FH)} e^{j[\tilde{\phi}^{(FH)} + \pi h \sum_{m=0}^{n-1} b^{(FH)}(m) + 2\pi h b^{(FH)}(n)q((iT_s - \tilde{\tau}^{(FH)})_T)]}
\end{aligned}
\tag{30}
$$

for $n = 0, 1, \cdots, N_{access} - 1$ and $i = 0, 1$, where N_{access} is the length of the known sequences carried by the FHSS signal; $\tilde{b}^{(DS)}(m)$ is the unknown information bits carried by the DSSS signal; $\tilde{\rho}^{(FH)}$, $\tilde{\phi}^{(FH)}$, and $\tilde{\tau}^{(FH)}$ are the unknown received timing, phase, and amplitude of the FHSS signal remained to be estimated; and the other variables were defined previously.

The corresponding one-shot estimation on the received timing, phase, and amplitude of the GFSK modulated FHSS signal based on MAP rule is

$$
(\hat{\tau}^{(FH)}(n), \hat{\phi}^{(FH)}(n), \hat{\rho}^{(FH)}(n)) = \arg \min_{\substack{b^{(DS)}(n - d_{1,0}) \\ b^{(DS)}(n - d_{1,1})}} \min_{\substack{\tau^{(FH)} \\ \phi^{(FH)} \\ \rho^{(FH)}}}
$$

$$
\sum_{i=0}^{1} |r(n,i) - \rho^{(DS)} e^{j\phi^{(DS)}} b^{(DS)}(n - d_{1,i}) \tilde{s}_1((iT_s - \tau^{(DS)})_T)
$$

$$
- \rho^{(FH)} e^{j[\phi^{(FH)} + \pi h \sum_{m=0}^{n-1} b^{(FH)}(m) + 2\pi h b^{(FH)}(n)q((iT_s - \tau^{(FH)})_T)]}|^2,
\tag{31}
$$

which is a joint estimation scheme of great complexity. In the sequel, we shall develop the suboptimum synchronizer with feasible complexity.

Since

$$\arg \min_{\substack{\tau^{(FH)} \\ \phi^{(FH)} \\ \rho^{(FH)}}} \sum_{i=0}^{1} |r(n,i) - \rho^{(DS)} e^{j\phi^{(DS)}} b^{(DS)}(n - d_{1,i}) \tilde{s}_1((iT_s - \tau^{(DS)})_T)$$

$$- \rho^{(FH)} e^{j[\phi^{(FH)} + \pi h \sum_{m=0}^{n-1} b^{(FH)}(m) + 2\pi h b^{(FH)}(n) q((iT_s - \tau^{(FH)})_T)]}|^2$$

$$= \arg \min_{\substack{\tau^{(FH)} \\ \phi^{(FH)} \\ \rho^{(FH)}}} \sum_{i=0}^{1} \{ -2Re\{ [r(n,i) - \rho^{(DS)} e^{j\phi^{(DS)}} b^{(DS)}(n - d_{1,i}) \tilde{s}_1((iT_s - \tau^{(DS)})_T)] \qquad (32)$$

$$exp\{ -j[\phi^{(FH)} + \pi h \sum_{m=0}^{n-1} b^{(FH)}(m) + 2\pi h b^{(FH)}(n) q((iT_s - \tau^{(FH)})_T)] \} \} + \rho^{(FH)} \},$$

the joint estimation of received timing, phase, and amplitude can be simplified to first estimate the received timing and phase. Moreover, the joint estimation of received timing and phase can be further simplified by implementing the non-coherent timing estimation designed by composite hypothesis testing. Thus

$$\hat{\tau}^{(FH)}_{non-coherent} = \arg \max_{\substack{b^{(DS)}(n - d_{1,0}) \\ b^{(DS)}(n - d_{1,1})}} \max_{\tau \in (-T_s, 0]} \{ [\sum_{i=0}^{1} Re\{ f(n,i) e^{-j[\pi h \sum_{m=0}^{n-1} b^{(FH)}(m) + 2\pi h b^{(FH)}(n) q((iT_s - \tau)_T)]} \}]^2$$

$$+ [\sum_{i=0}^{1} Im\{ f(n,i) e^{-j[\pi h \sum_{m=0}^{n-1} b^{(FH)}(m) + 2\pi h b^{(FH)}(n) q((iT_s - \tau)_T)]} \}]^2 \},$$

$$(33)$$

where $f(n,i) \equiv r(n,i) - \rho^{(DS)} e^{j\phi^{(DS)}} b^{(DS)}(n - d_{1,i}) \tilde{s}_1((iT_s - \tau^{(DS)})_T)$; $Re\{x\}$ and $Im\{x\}$ are the real and imaginary part of x in the complex filed; and $\hat{\tau}^{(FH)}_{non-coherent}(n)$ is the non-coherent timing estimation of the FHSS signal.

Remarks:

- Please note that the chosen $b^{(DS)}(n - d_{1,0})$ and $b^{(DS)}(n - d_{1,1})$ are the estimates of the information bits of the DSSS signal. With these estimates, it is easy to estimate the received phase and amplitude of the FHSS signal.

- The estimated $\hat{\tau}^{(FH)}_{non-coherent}(n)$, $\hat{\phi}^{(FH)}(n)$, and $\hat{\rho}^{(FH)}(n)$ can be averaged over $n = 0, 1, \cdots, N_{access} - 1$ to obtain a better estimate of the received timing, phase, and amplitude of the FHSS signal.

19

Figure 8 elaborates the dashed box in Figure 7 and thus completes the design of the FHSS signal demodulation in the Bluetooth and IEEE 802.11b devices. As could be seen in Figure 8(b), the number of branches needed in the non-coherent timing estimation is $B^2 N_\tau$, where N_τ is the number of timing candidates within half a symbol duration and B is the number of possible values of $b^{(DS)}(n) \; \forall \; n$. (e.g. $B = 2$ when the IEEE 802.11b employs BPSK modulation; $B = 4$ when the QPSK modulation is employed.) In fact, the complexity of the non-coherent timing estimation could be further reduced to be $B N_\tau$, if we correlate the received signal within a symbol of the DSSS signal instead of the FHSS signal. We shall elaborate the design in the sequel.

Since we assume the knowledge of received timing of the DSSS signal, we always could properly set the origin of the coordinate such that $\tau^{(DS)} \in (-T_s, 0]$. In this case, the over-sampled sequence

$$
\begin{aligned}
r(n, i) &\equiv r_{LP}(nT + iT_s) \\
&= \rho^{(DS)} e^{j\phi^{(DS)}} \tilde{b}^{(DS)}(n) \tilde{s}_1(iT_s - \tau^{(DS)}) + z(n, t) \\
&\quad + \tilde{\rho}^{(FH)}(nT + iT_s - \tilde{\tau}^{(FH)}) e^{j[\tilde{\phi}^{(FH)} + \pi h \sum_{m=0}^{n-d_i-1} b^{(FH)}(m) + 2\pi h b^{(FH)}(n-d_i)q((iT_s - \tilde{\tau}^{(FH)})\tau)]}
\end{aligned}
\tag{34}
$$

where $d_i = \beta$ if $-\beta T \leq iT_s - \tilde{\tau}^{(FH)} < (1 - \beta)T$ and $b^{(FH)}(m) = 0$ for $m < 0$. With a coarse timing estimation, we could have either $\tilde{\tau}^{(FH)} \in [0, T_s)$ or $\tilde{\tau}^{(FH)} \in [T_s, T)$, and the corresponding one-shot timing estimation of the FHSS signal with random phase is

$$
\begin{aligned}
\hat{\tau}^{(FH)}_{non-coherent} &= \arg \max_{b^{(DS)}(n)} \max_{\tau} \{ [\sum_{i=0}^{1} Re\{ g(n, i) e^{-j[\pi h \sum_{m=0}^{n-d_i-1} b^{(FH)}(m) + 2\pi h b^{(FH)}(n-d_i)q((iT_s - \tau)\tau)]} \}]^2 \\
&\quad + [\sum_{i=0}^{1} Im\{ g(n, i) e^{-j[\pi h \sum_{m=0}^{n-d_i-1} b^{(FH)}(m) + 2\pi h b^{(FH)}(n-d_i)q((iT_s - \tau)\tau)]} \}]^2 \},
\end{aligned}
\tag{35}
$$

where $g(n, i) \equiv r(n, i) - \rho^{(DS)} e^{j\phi^{(DS)}} b^{(DS)}(n) \tilde{s}_1((iT_s - \tau^{(DS)})_T)$.

Figure 9 depicts the block diagram of the new non-coherent timing estimation of the FHSS signal interfered by a DSSS signal. To ease the illustration, we consider the DSSS signal employing BPSK modulation. $\tau^{(n)}$ for $n = 0, 1, \cdots, N_\tau - 1$ are the timing candidates to estimate the received timing of the FHSS signal. And $d_i^{(n)} = \beta$ provided $-\beta T \leq iT_s - \tau^{(n)} <$

20

$(1 - \beta)T$. The number of correlators needed in this design is BN_r comparing to the $B^2 N_r$ correlators needed in Figure 8(b).

Figure 7 is not the only mechanism to implement the *Identification block* and *Synchronization block* in Figure 5. An alternative is plotted Figure 10. The rationale behind this alternative is to also receive the consecutive channels of the target one as shown in Figure 11. With this extra side information which contains the interfering DSSS signal, we can avoid the performance degradation of Figure 7 when the DSSS signal is detected later than $-t_2$.

5.2 Linear Interference Suppression Detection on 802.11b Devices

Due to the wide band occupied by the DSSS signal, the considered number of FHSS interferences is usually larger than 1. In addition, we could no longer ignore the possibility that these FHSS signals hop into the same frequency band. Therefore, in the reception of the IEEE 802.11b devices in the coexistent environment, we consider L interfering FHSS signals and these FHSS signals may collide. The corresponding received lowpass equivalent signal $r_{LP}(t)$ is

$$
\begin{aligned}
r_{LP}(t) = &\sum_{m=0}^{M-1} b^{(DS)}(m) s_1(t - mT) \rho^{(DS)} e^{j\phi^{(DS)}} + z_{LP}(t) \\
&+ \sum_{n=0}^{N-1} \sum_{l=1}^{L} [\rho_{2l-1}^{(FH)}(n) s_{2l}(t - \tau_l^{(FH)} - nT) \\
&+ \rho_{2l}^{(FH)}(n) s_{2l+1}(t - \tau_l^{(FH)} - nT)].
\end{aligned}
\tag{36}
$$

Again, applying the sampling theorem, we over-sample $r_{LP}(t)$ at rate $1/T_{sc} \equiv 2/T_c$, where T_c is the chip duration. Please note that the sampling rate in the DSSS signal is much higher than the one in the FHSS signal.

$$
\begin{aligned}
r(m,n,i) \equiv &\, r_{LP}(mT + nT_c + iT_{sc} + \tau) \\
= &\, b^{(DS)}(m) s_1((nT_c + iT_{sc} + \tau)_T) \rho^{(DS)} e^{j\phi^{(DS)}} + z(m,n,i) \\
&+ \sum_{l=1}^{L} [\rho_{2l-1}^{(FH)}(m - d_{l,n,i}) s_{2l}((nT_c + iT_{sc} + \tau - \tau_l^{(FH)})_T) \\
&+ \rho_{2l}^{(FH)}(m - d_{l,n,i}) s_{2l+1}((nT_c + iT_{sc} + \tau - \tau_l^{(FH)})_T)],
\end{aligned}
\tag{37}
$$

21

where $d_{i,n,j} = \beta$ if $-\beta T \leq nT_c + iT_{sc} + \tau - \tau_l^{(FH)} < (1-\beta)T$; τ is a known timing misalignment ($\tau \in [0, T_{sc})$); and β is an integer.

The block diagram of the linear interference suppression detection for IEEE 802.11b devices is therefore as shown in Figure 12. The number of correlators required is $2L+1$ and the combination coefficients can be calculated beforehand to save the system complexity if we adopt the decorrelating-type design criterion. The complete block diagram of the receiver is similarly as in Figure 5 with the dashed box replaced by Figure 12. And it remains to design the *Identification block* and the *Synchronization block* for IEEE 802.11b devices. The *Identification block* is used to identify the number of FHSS signals while the *Synchronization block* estimates the received timing, phase, and amplitude of both the DSSS signal and the FHSS signals.

6   Conclusions

Previous technique on multiuser detection was used to mitigate the interference from other DSSS signals. In this paper, we extend its ability to mitigate the interference from FHSS signals and/or DSSS signals. In addition, the known linear multiuser detection is limited to the linearly modulated signals and we extend its ability to even the non-linearly modulated signals.

These theoretical designs are further demonstrated in the practical applications that the IEEE 802.11b and Bluetooth devices collocated in the same unlicensed 2.4 GHz band. With the practical considerations of the IEEE 802.11b and Bluetooth coexistent environment, the complete receivers including the synchronizers and detectors to effectively suppress the interference were proposed for both the Bluetooth and IEEE 802.11b devices.

In fact, the ability of the proposed linear interference suppression detection is not limited to the IEEE 802.11b and Bluetooth coexistent environment. As long as we could retrieve the information of the interference, our proposed detection can effectively suppress the interference.
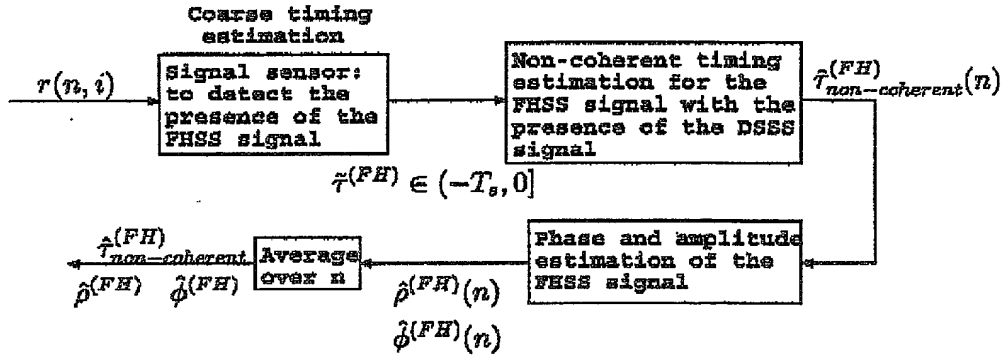
References

[1] Rajiv Vijayan and H. Vincent Poor, "Nonlinear techniques for interference suppression in spread-spectrum systems," *IEEE Trans. on Communications*, vol. 38, no. 7, pp. 1060-1065, July 1990.

[2] Catharina Carlemalm, H. Vincent Poor, and Andrew Logothetis, "Suppression of multiple narrowband interferers in a spread-spectrum communication system," *IEEE Journal on Selected Areas in Communications*, vol. 18, no. 8, pp. 1365-1374, August 2000.

[3] Slim Souissi and John B. Gehman, "Method and apparatus for interference suppression in spread spectrum signals," *United States Patent 5,671,247*, September 23, 1997.

[4] Chad Scott Bergstorm, Jeffrey Scott Chuprun, and John Eric Kleider, "Method and apparatus for performing frequency hopping adaptation," *United States Patent 6,118,805*, September 12, 2000.

[5] S. Verdu, "Minimum probability of error for asynchronous Gaussian multiple access channels," *IEEE Trans. Inform. Theory*, vol. IT-32, pp. 85-96, Jan. 1986.

[6] R. Lupas, S. Verdu, "Near-far resistance of multiuser detectors in asynchronous channels," *IEEE Trans. Communications*, vol. 38 , pp 496-508, April, 1990.

[7] R. Lupas and S. Verdu, "Linear multiuser detectors for synchronous code-division multiple-access channels," *IEEE Trans. Information Theory*, vol. 35, no. 1, pp. 123-136, Jan. 1989.

[8] Zhenhua Xie, Robert T. Short, and Craig K. Rushforth, "A family of suboptimum detectors for coherent multiuser communications," *IEEE Journal on Selected Areas in Communications*, vol. 8. no. 4, May 1990.

[9] Hertz David and Greenberger Harvey J. "Asynchronous CDMA decorrelating detector," *United States Patent 5,917,829*, June 29, 1999.
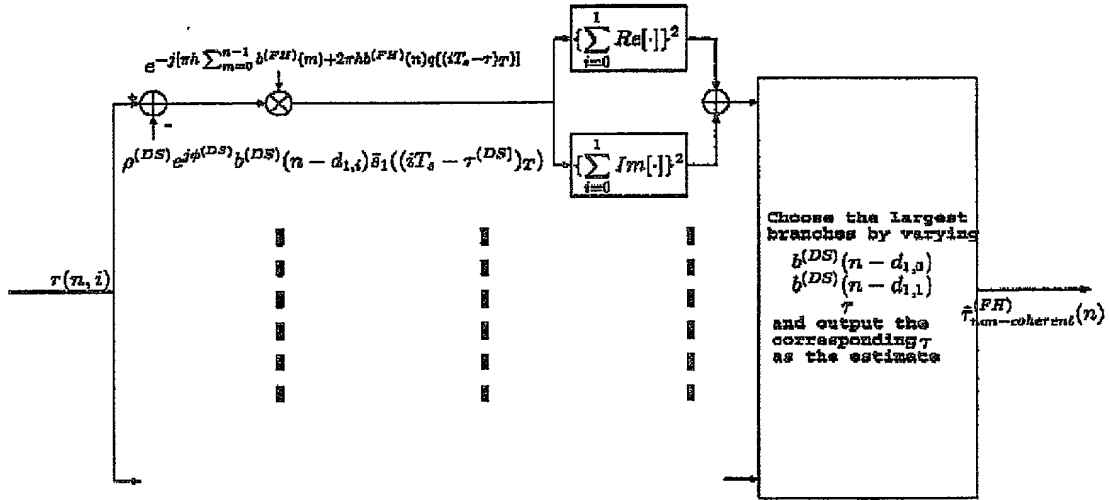
23

[10] Cha'o-Ming Chang and Kwang-Cheng Chen, "Multiuser Synchronization," in Proc. IEEE PIMRC, Sept. 2000, pp. 1090-1095. (invited)

[11] *Specification of the Bluetooth System, v1.0 B*, Dec. 1999.

Coarse timing estimation

$r(n, i)$ → | Signal sensor: to detect the presence of the FHSS signal | → | Non-coherent timing estimation for the FHSS signal with the presence of the DSSS signal | → $\tilde{\tau}^{(FH)}_{non-coherent}(n)$

$\tilde{\tau}^{(FH)} \in (-T_s, 0]$

$\hat{\tau}^{(FH)}_{non-coherent}$, $\hat{\rho}^{(FH)}$ $\hat{\phi}^{(FH)}$ ← | Average over n | ← $\hat{\rho}^{(FH)}(n)$, $\hat{\phi}^{(FH)}(n)$ ← | Phase and amplitude estimation of the FHSS signal |

(a) Block diagram of the synchronization for the FHSS signal

$e^{-j[\pi h \sum_{m=0}^{n-1} b^{(FH)}(m) + 2\pi h b^{(FH)}(n)q((iT_s - \tau)T)]}$

$\{\sum_{i=0}^{1} Re[\cdot]\}^2$

$\{\sum_{i=0}^{1} Im[\cdot]\}^2$

$\rho^{(DS)} e^{j\phi^{(DS)}} b^{(DS)}(n - d_{1,i}) \tilde{s}_1((iT_s - \tau^{(DS)})T)$

$r(n, i)$

| Choose the largest branches by varying $b^{(DS)}(n - d_{1,0})$ $b^{(DS)}(n - d_{1,1})$ τ and output the corresponding τ as the estimate |

$\tilde{\tau}^{(FH)}_{non-coherent}(n)$

(b) Non-coherent timing estimation
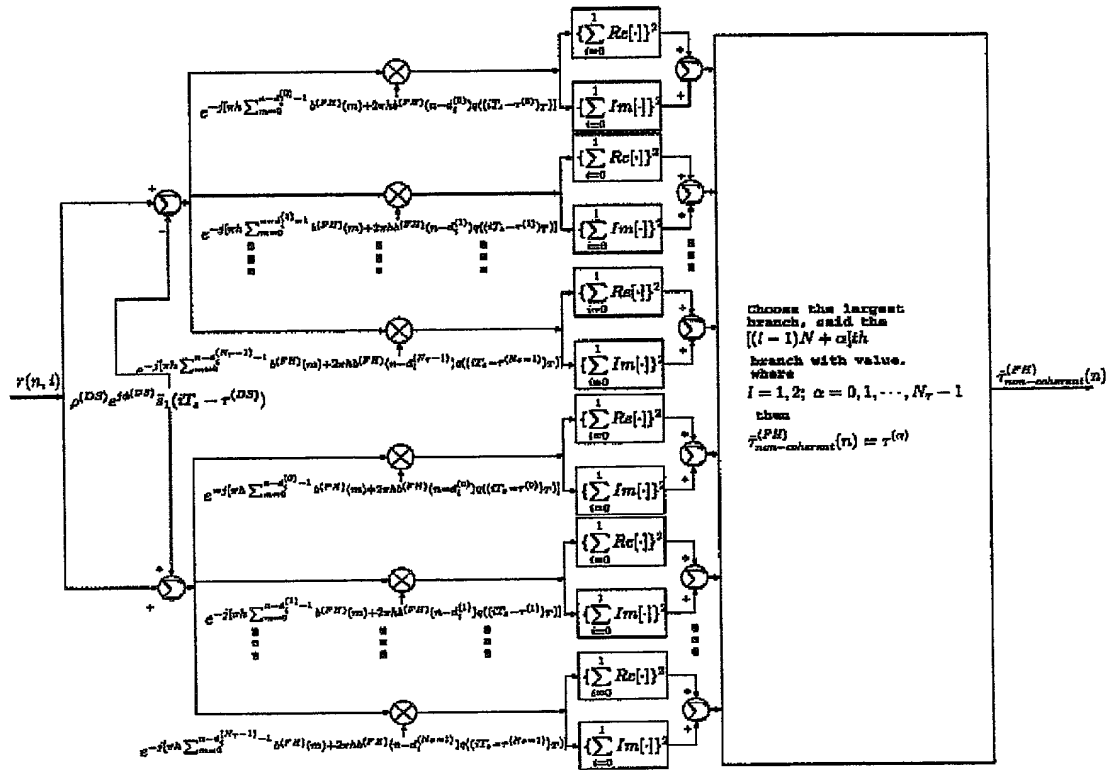
Figure 8: The dashed box in Figure 7.

Figure 9: Non-coherent timing estimation as an alternative to Figure 8(b)
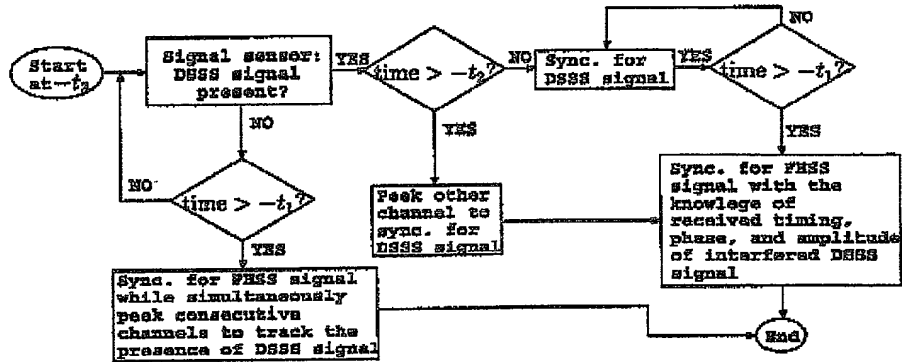
Figure 10: Flow diagram of the Bluetooth synchronizer by peeking consecutive channels
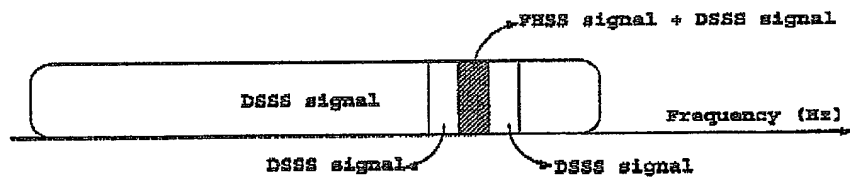

Figure 11: An illustrative plot of the new synchronization mechanism.

$s_1(n,i) \equiv s_1((nT_c + iT_{sc} + \tau)_T)$

$s_{2l}(n,i) \equiv s_{2l}((nT_c + iT_{sc} + \tau - \tau_l^{(FH)})_T)$

$s_{2l+1}(n,i) \equiv s_{2l+1}((nT_c + iT_{sc} + \tau - \tau_l^{(FH)})_T)$

$l = 1, 2, \cdots, L$

$A_{i,j}$ is the entry of A in its ith row and jth column.

A is the $(4L+1) \times (4L+1)$ matrix designed according to different criteria.
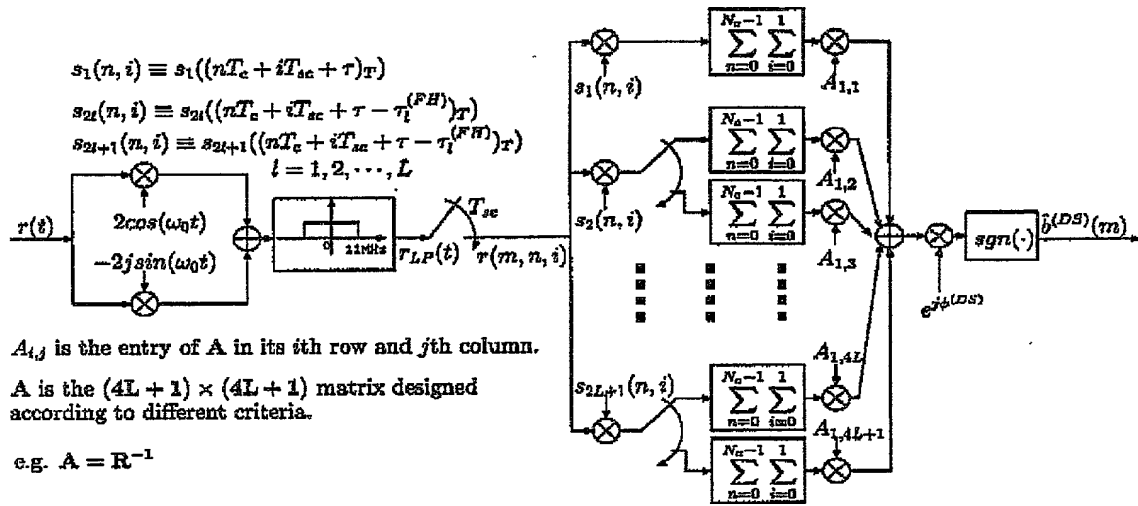
e.g. $A = R^{-1}$

Figure 12: Block diagram of linear interference suppression detection on 802.11b devices